Drag, lift and torque coefficients for ellipsoidal particles

Mohammed Khalij, R Ouchene, A Tanière, B Arcen

Drag, lift and torque coefficients for ellipsoidal particles

R. Ouchene[a], M. Khalij[a], A. Tanière[a], B. Arcen[b]

[a] *CNRS, LEMTA, UMR 7563, Université de Lorraine – ESSTIN, 2 rue Jean Lamour, 54500 Vandoeuvre-les-Nancy, France.*

[b] *CNRS, LRGP, UMR 7274, Université de Lorraine, Nancy, F-54000, France.*

Abstract. In this work, we want to verify the ability of the CFD code Ansys Fluent© to give an accurate prediction of hydrodynamic forces acting on non-spherical (Ellipsoids). We focus the present study only on the drag and lift forces and also on the pitching torque. The objective is to choose or develop a model that will later be introduced in a Direct Numerical Simulation code coupled with a particles Lagrangian tracking in order to study the dispersion of non-spherical particles.

Keywords: Non spherical particles, drag, lift, torque, correlations

INTRODUCTION

Non-spherical particles shapes are more and more considered in the modeling and simulation of a variety of engineering applications such as cyclone separator, coal combustion or pulp and paper. A complete description of the behavior of these particles requires the modeling of the translational and rotational motion of particles tacking its orientation into account, in contrast to the spherical particle case.

Several studies have been performed over the past 20 years, but they are mainly devoted to the drag force acting on non-spherical particles. Chhabra *et al.* [1] were the first to compile and classify the most used correlations. According to their study they showed that the correlation derived by Ganser [2] is the most accurate. They distinguished two types of approach that have been used in later studies. The first one is to define a single correlation for all shapes and orientations (Tran-Cong *et al.* [3], Yow *et al.* [4], Hölzer & Sommerfeld [5]). Indeed, Tran-Cong *et al.* [3] proposed a correlation from their experimental data obtained from agglomerates of ordered packed spheres. Yow *et al.* [4] used data available in the literature to extract a new correlation which unfortunately, does not take the particle orientation into accounts. This parameter was introduced in the correlation of Hölzer & Sommerfeld [5], through two shape parameters which are sphericity [6] and crosswise sphericity. The second approach consists in obtaining a drag coefficient expression for a fixed shape and orientations. Rosendahl[7] suggested to determine the drag coefficient at two incidences angles ,*i.e.* 0° and 90° $\left(C_{D,\alpha=0°}, C_{D,\alpha=90°}\right)$, from the best experimental results or from existing correlations. Then, a function linking these two limiting cases, with an inflection point at 45 °, is used to represent the whole range of incidence angles for a non-spherical particle. A similar approach was used by Zastawny *et al.* [8], nonetheless they determined $C_{D,\alpha=0°}$ and $C_{D,\alpha=90°}$ using their new correlation issued from data simulations. In this study, we are interested in the second approach which is more accurate that the first one. Unlike the drag coefficients, there are few studies devoted to the lift and torque coefficients in the literature. An interesting study was proposed by Yin *et al.* [9], who assumed, like Hoener [10], that the lift coefficient is proportional to the drag one, nevertheless Zastawny *et al.* [8] showed the weakness of this assumption. Moreover, generally, the pitching torque is obtained by a combination of drag and lift forces acting on the center of pressure which is not coincident with the gravity center. The only formula of the torque coefficient was given by Zastawny *et al.* [8] for specific particles shapes.

We propose in this paper to examine the ability of the industrial CFD code Ansys Fluent© to provide the hydrodynamic forces acting on non-spherical particles (ellipsoids). We will present the drag and lift forces and torque. The objective is to have a clear opinion about correlations that will be used in our Direct Numerical Simulation code coupled with a Lagrangian tracking DNS / DPS in order to study the dispersion of non-spherical particles.

The document is organized in three sections. The first one is devoted to the description of the model of the motion of non-spherical particles and the main available correlations. In the second section, the numerical simulations are presented with the validation cases. Then, the results for the non-dimensional hydrodynamics parameters are given and discussed in section four before the conclusions.

Motion of a non-spherical particle

There are few models that describe the motion of non spherical particles suspended in a fluid flow. Indeed, this type of particles is not only subject to translation forces but also to rotational motion around themselves. The translational motion of a particle is described in the reference inertial x = (x, y, z) by the conservation of momentum. In addition, for "heavy" solid particles only the drag F_D, lift F_L and volume forces are predominant (eq.1) [11]:

$$m_p \frac{d\vec{u}_p}{dt} = \vec{F}_D + \vec{F}_L + V_p\left(\rho_p - \rho_f\right)\vec{g}\,, \tag{1}$$

where V_p , ρ_p, ρ_f, represent respectively the volume of the particle, the density of the particle and the density of the fluid.

The rotational motion for non spherical particles is induced by the different location of the center of mass and the center of pressure. Therefore, and an additional torque is added and the following equations have to be solved:

$$\begin{cases} I_{x'}\dfrac{d\omega_{x'}}{dt} - \omega_{y'}\omega_{z'}\left(I_{y'} - I_{z'}\right) = T_{x'} \\ I_{y'}\dfrac{d\omega_{y'}}{dt} - \omega_{z'}\omega_{x'}\left(I_{z'} - I_{x'}\right) = T_{y'}\,, \\ I_{z'}\dfrac{d\omega_{z'}}{dt} - \omega_{x'}\omega_{y'}\left(I_{x'} - I_{y'}\right) = T_{z'} \end{cases} \tag{2}$$

where $I_{x`}$, $I_{y`}$, $I_{z`}$ represent the moment of inertia; $\omega_{x`}$, $\omega_{y`}$, $\omega_{z`}$ are the angular velocities according to (x', y', z') and $T_{x`}$, $T_{y`}$, $T_{z`}$ are the torque relative to the three directions.

Usually, the forces acting on a non-spherical particle are characterized by the dimensionless drag C_D, lift C_L and torque C_T coefficients which depend on the particle Reynolds number $\mathrm{Re}_p = \|\vec{u}_R\| d_p / \nu$, where $\vec{u}_R = \vec{v}_p - \vec{u}_f$ is the relative velocity between the particle and the fluid, $\vec{u}_f$ and $\vec{v}_p$ represent respectively the velocity of the particle and the velocity of the fluid, d_p is the diameter equivalent sphere, and ν is the kinematic viscosity of the fluid. Thus, these coefficients are obtained using the following formulations:

$$C_D = \frac{F_D}{\frac{1}{2}\rho_f {u_R}^2 \frac{\pi}{4} d_p^2}\,; C_L = \frac{F_L}{\frac{1}{2}\rho_f {u_R}^2 \frac{\pi}{4} d_p^2}\,; C_T = \frac{T_P}{\frac{1}{2}\rho_f {u_R}^2 \frac{\pi}{8} d_p^3}\,. \tag{3}$$

For a particle which is not symmetric (unlike the sphere), the drag and lift coefficients depend not only on particle Reynolds number but also on their incidence angle α with respect to the flow (Fig. 1). This effect plays an important role in the motion of non-spherical particles [10] through the drag and lift forces. Hence, for an accurate description of the non spherical particles motion, the drag, lift and torque coefficients have to be precisely predicted. Table.1 reports the correlations that will be compared to the results obtained by numerical simulations in order to assess their accuracy.

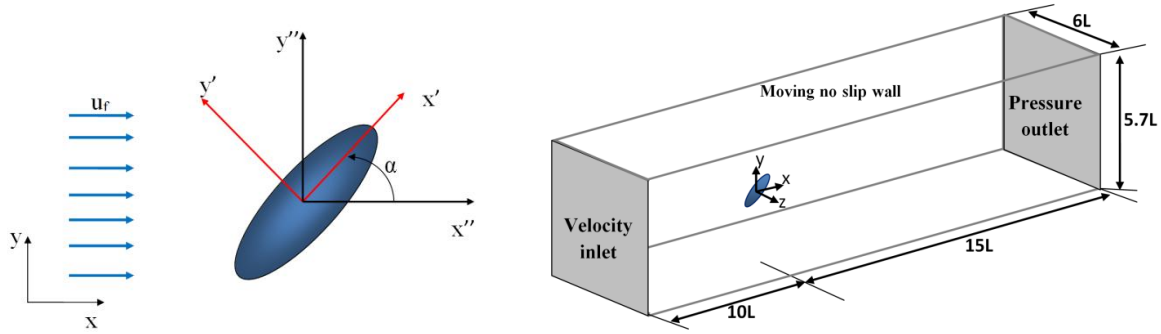

Figure 1.Geometrical configuration and boundary conditions. (x, y, z), (x', y', z') are respectively co-moving and co-rotating frames of references.

Table (1). Reference correlations.

Authors	Correlations
Hölzer & Sommerfeld [5]	$C_D = \frac{8}{Re_p}\frac{1}{\sqrt{\phi_\perp}} + \frac{16}{Re_p}\frac{1}{\sqrt{\phi}} + \frac{3}{\sqrt{Re_p}}\frac{1}{\phi^{\frac{3}{4}}} + 0.42*10^{0.4(-\log\phi)^{0.2}}\frac{1}{\phi_\perp}$
Rosendahl [7]	$\begin{cases} C_D = C_{D,\alpha=90°} + \left(C_{D,\alpha=90°} - C_{D,\alpha=0°}\right)\sin^3\alpha \\ \text{Where :} \\ C_{D,\alpha=0°} = \frac{8}{Re_p}\frac{1}{\sqrt{\phi_\perp}} + \frac{16}{Re_p}\frac{1}{\sqrt{\phi}} + \frac{3}{\sqrt{Re_p}}\frac{1}{\phi^{\frac{3}{4}}} + 0.42*10^{0.4(-\log\phi)^{0.2}}\frac{1}{\phi_\perp} \\ C_{D,\alpha=90°} = \frac{8}{Re_p}\frac{1}{\sqrt{\phi_\perp}} + \frac{16}{Re_p}\frac{1}{\sqrt{\phi}} + \frac{3}{\sqrt{Re_p}}\frac{1}{\phi^{\frac{3}{4}}} + 0.42*10^{0.4(-\log\phi)^{0.2}}\frac{1}{\phi_\perp} \end{cases}$
Zastawny *et al* [8]	$\begin{cases} C_D = C_{D,\alpha=90°} + \left(C_{D,\alpha=90°} - C_{D,\alpha=0°}\right)\sin^{a_0}\alpha \\ \text{Where :} \\ C_{D,\alpha=0°} = \frac{a_1}{Re_p{}^{a_2}} - \frac{a_3}{Re_p{}^{a_4}} \\ C_{D,\alpha=90°} = \frac{a_5}{Re_p{}^{a_6}} - \frac{a_7}{Re_p{}^{a_4}} \end{cases}$ $C_L = \left(\frac{b_1}{Re_p{}^{b_2}} - \frac{b_3}{Re_p{}^{b_4}}\right)\sin(\alpha)^{b_5+b_6Re_p{}^{b_7}}\cos(\alpha)^{b_8+b_9Re_p{}^{b_{10}}}$ $C_M = \left(\frac{c_1}{Re_p{}^{c_2}} - \frac{c_3}{Re_p{}^{c_4}}\right)\sin(\alpha)^{c_5+c_6Re_p{}^{c_7}}\cos(\alpha)^{c_8+c_9Re_p{}^{c_{10}}}$
Hoener [10]	$\frac{C_L}{C_D} = \sin^2\alpha\cos\alpha$

NUMERICAL SIMULATION

We want to examine the hydrodynamic forces acting on ellipsoidal particles. The particle is supposed fixed and immerged in a tridimensional uniform flow. Then, the relative velocity is equal to the fluid velocity $\vec{u}_f$. Simulations are performed using the CFD code Ansys Fluent©. Centered scheme are used for discretizing all the numerical fluxes in the Navier–Stokes equations. The problem of the coupling between velocity and pressure is tackled with a Semi-Implicid Method for Pressure-Linked Equations (SIMPLE) [12]. The geometrical configuration (Fig.1) is a parallelepiped (fluid box) surrounding the particle. The dimensions of the box are given as a function of *L* in Fig.1. They were determined to prevent any disturbance of the flow due to boundary conditions, particularly in the boundary layer. From a practical point of view, these dimensions were imposed by the case Re_p = 0.1 resulting in a greater boundary layer where the particle is positioned transversely to the flow. In addition, the length of the computational box was set to leave an adequate distance for the development of the wake. The mesh of the fluid

domain consists of tetrahedral elements. The mesh surface of the particle is sufficiently fine to give an accurate integration of the stresses acting on the particle surface. Thus, the number of cells is about 500 000. The boundary layer is always represented by at least 20 nodes.

The boundaries conditions are presented in Fig.1. A constant velocity inflow condition is imposed at the inlet boundary whereas homogeneous Neumann conditions are chosen at the outlet and Moving No-slip condition are specified on lateral boundaries.

Table (2). Particles shapes

Ellipsoid w=5/1	Ellipsoid w=5/2	Ellipsoid w=5/4
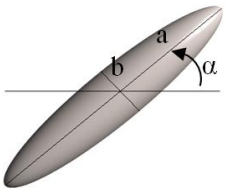	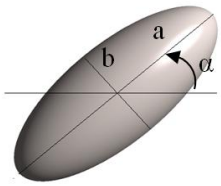	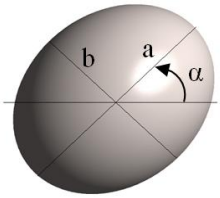

In order to anticipate the effects of the unsteady flow, we performed some simulations under the steady and unsteady flow conditions for $\alpha = 40°$. The results of these simulations were identical for the both conditions. Then, we ran all the other simulations (See Tab.3) under the steady flows conditions.
Before to examine the results obtained for the ellipsoidal particles given in (Tab.2), we present the drag coefficient for a sphere and an ellipsoid with an aspect ratio w=5/2 at low particle Reynolds number in order to validate our computational methodology.

- The first one is the case of a sphere in a Stokes flow regime. The numerical result of the drag coefficient obtained at Re_p = 0.1 is: C_D=245 knowing that the theoretical result is C_D=24/ Re_p=240. A deviation of 2% is obtained.
- The second case is performed with an ellipsoid in a Stokes flow regime and the results are compared to the analytical solution of Brenner [13], the deviation is of 3 %. (See: Fig.2).

These deviations can be explained by the infinite fluid domain assumption which cannot be reproduced in our simulation. Nonetheless, the obtained results show the good accuracy of the numerical prediction of the drag forces acting on fixed particles. We also reported the results of Zastawny *et al.* [8], the deviation from theoretical results is more pronounced. We believe that the spatial resolution used by Zastawny *et al.* [8] is too low to correctly predict this case.

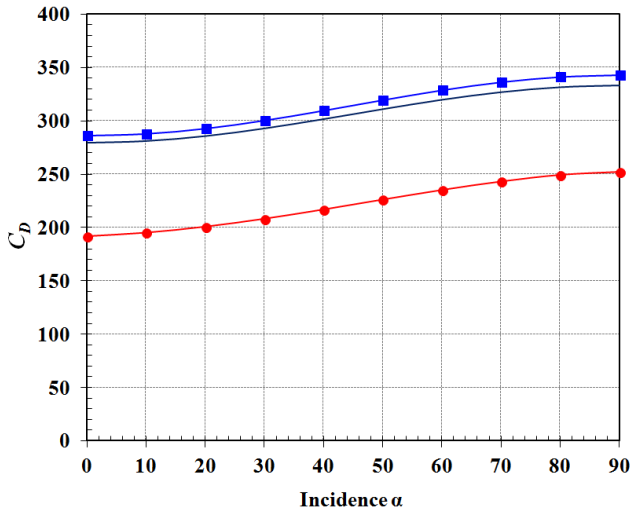

Figure 2. Drag coefficient obtained for the ellipsoid w=5/2 at Re_p = 0.1. Present results: (—■—); theoretical results of Brenner [13]: (——); Results of Zastawny *et al.* [8] are also reported (—●—).

Table (3). Parameters of the simulations.

Re_p	Particle	Ratio $w=L/D$	Orientation α
10, 50, 240, 300	Ellipsoid	5/1, 5/2, 5/4	0 to 90°

RESULTS AND DISCUSSION

Simulations were performed to compute the drag C_D, lift C_L and torque C_T coefficients for ellipsoidal particles at different angles of incidence and for different particle Reynolds numbers. Several aspect ratios were tested (see Tab.2). The results of calculation are reported in Figs. (3-6) and compared with the correlations of Hölzer & Sommerfeld [5], Rosendahl [7] and Zastawny *et al.* [8] given in Tab.1. It has to be noted that the value of $C_{D,\alpha=0°}$, and $C_{D,\alpha=90°}$, used for the correlation of Rosendahl [7] were computed from the correlation of Hölzer & Sommerfeld [5].

Drag coefficients are presented on the left of the Fig.3 as a function of incidence angles. Zastawny *et al*. [8] results are not presented for the case w=5/1 since they did not consider this one. The results are qualitatively in good agreement with those issued from the literature since a similar trend is observed, the drag coefficient increases for increasing incidence angles whatever the value of aspect ratio and particle Reynolds number. A horizontal tangent is present at α=90°due to the symmetry of the curves relative to the axis α=90° whatever the treated case. An inflection point at α=45° is noticed, this is a characteristic specificity of this kind of particles. Note that this inflection point is not reproduced by the correlation of Hölzer & Sommerfeld [5]. For highest particle Reynolds number (Re_p = 300), the results of our simulations show good agreement with the results of Zastawny *et al*. [8] for w=5/2. Nonetheless, for w=5/4, a better agreement is noticed with the correlations of Hölzer & Sommerfeld [5] and Rosendahl [7]. For Re_p = 10, there is a great disparity in results. The difference between our values and those obtained by Zastawny *et al*. [8] is about 30%. A possible explanation would be that the correlation of Zastawny'results is not accurate at low particle Reynolds number as already mentioned. For this low particle Reynolds number value, our results are in better accordance with those of Hölzer & Sommerfeld [5] and Rosendahl [7]. In view of the present results for the drag coefficient, we will choose the method proposed by Rosendahl [7], i.e. use the C_D's values at 0° and 90 ° and then, linking them by a trigonometric function. The values of the drag coefficient at 0° and 90° will be extracted from Hölzer & Sommerfeld [5]'s correlation.

The lift coefficient C_L which is presented as a function of particle Reynolds number is shown on the right in Fig. 3. Whatever the aspect ratio, it has to be observed that the values of the lift coefficients are higher for Re_p = 10 than for Re_p = 300, as noticed before for C_D. As it can be seen in Fig. 3, the computed lift coefficient increases to a maximum located near an incident angle of α=45°and then decreases. Similar trends are obtained by Zastawny *et al*. [8]. The evolution of C_L predicts by Hoener [10] does not coincide with our results and those obtained by Zastawny *et al*. [8]. Moreover, the maximum lift coefficient predicted by Hoener [10] is located at α=60° while we found $\alpha = 45°$. Considering the drag and lift coefficient results, it can be concluded as Hoener [10] and Zastawny *et al.* [8] that the lift coefficient cannot be only a function of incidence angle α and drag coefficientC_D.

Finally, it is clear that our results are in better agreement with those obtained by Zastawny *et al.* [8] than with the correlation of Hoener [10]. Therefore, the correlation of C_L proposed by Zastawny *et al.* [8] will be chose even if a maximum error of about 30 % can be noted for low particle Reynolds number.

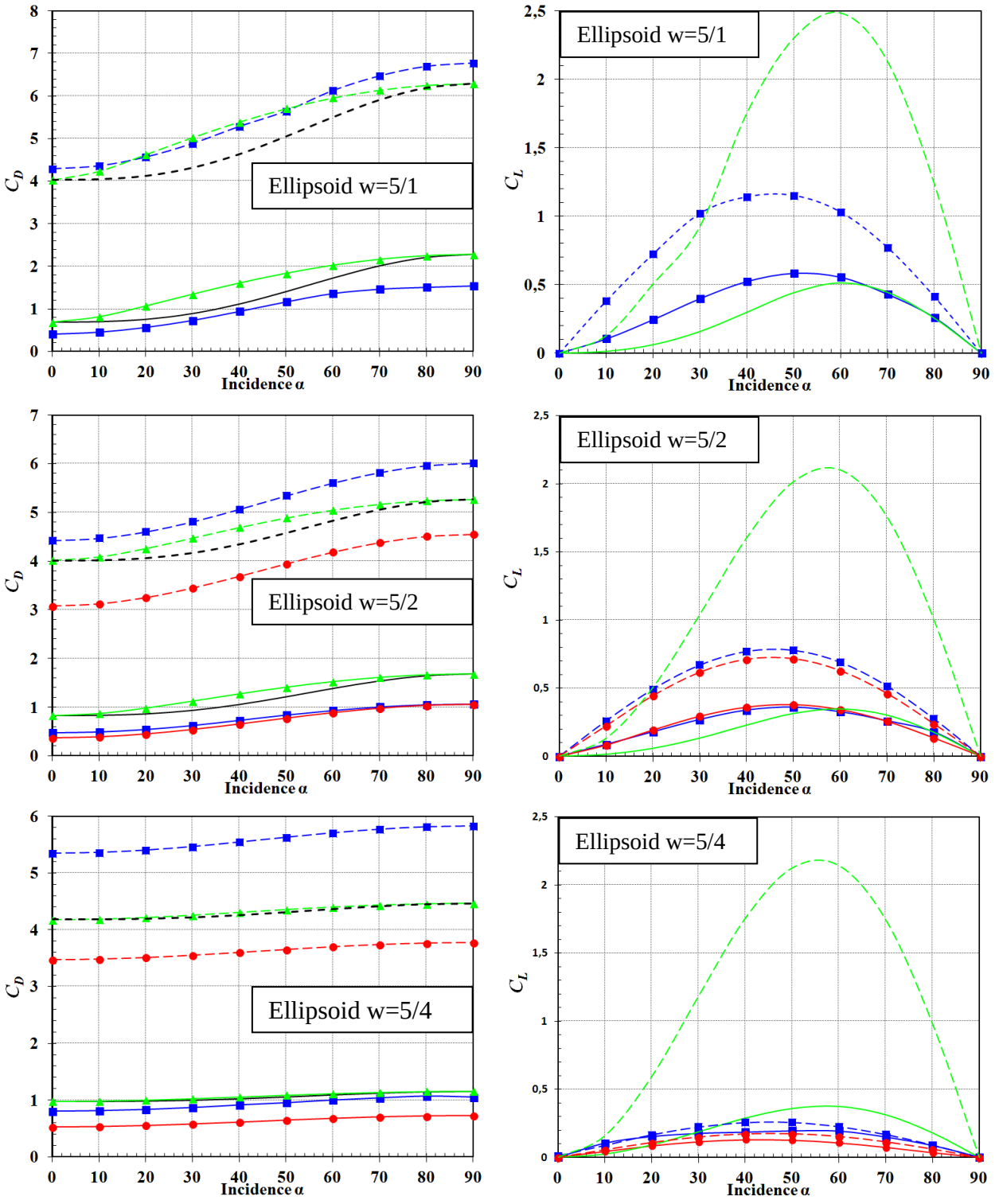

Figure 3. Comparison of the computed drag and lift coefficients with the existing correlations for different particles Reynolds numbers. On the left, drag coefficients and on the right lift coefficients as a function of the angle of incidence α. (——): Rosendahl [7]; (—■—): Ansys Fluent©; (—●—): Zastawny *et al.* [8];(—▲—): Hölzer & Sommerfeld. [5]; (——): Hoener. [10]. The dashed lines are referred to Re_p = 10 and the continuous lines are referred to Re_p = 300.

In the following figure (Fig. 4), additional results are shown concerning the evolution of the computed normalized drag coefficients $C_D/C_{D,\alpha=90°}$ as a function of α for different aspect ratio and particle Reynolds numbers. Whatever the values of the particle Reynolds number, a same trend is retrieved *i.e.* a monotonic increase as incidence angle increases with an inflexion point at α=45°. A limit seems to be reached when Re_p is higher than 240 whatever the aspect ratio. It is show clearly that the influence of incidence angle has a less influence on $C_D/C_{D,\alpha=90°}$, for the lowest aspect ratio (w=5/4 near to a spherical shape) comparing to the other ones. In order to better understand such a behavior, we have analyzed the contribution of the pressure and friction drag (the total drag force is the sum of pressure and friction drag forces). In Fig. 5, we present the pressure and friction drag coefficients normalized by $C_{D,\alpha=90°}$, as a function of the incidence angle for two values of Re_p (10 and 300). The evolution of the pressure drag coefficient is similar to that of the total normalized drag coefficient whereas the friction drag coefficient is not sensitive to the incidence angle. Therefore, the evolution of total drag coefficient as a function of α is mainly due to the pressure drag coefficient contribution, whatever the value of the particle Reynolds number. We can also remark in the same figure the influence of Re_p on the values of the pressure and friction drag coefficients. In contrast to the pressure contribution, the friction drag coefficient is significantly influenced by the particle Reynolds number whatever the aspect ratios and incidence angle. At Re_p = 300, the friction drag is half the value obtained at Re_p = 10.

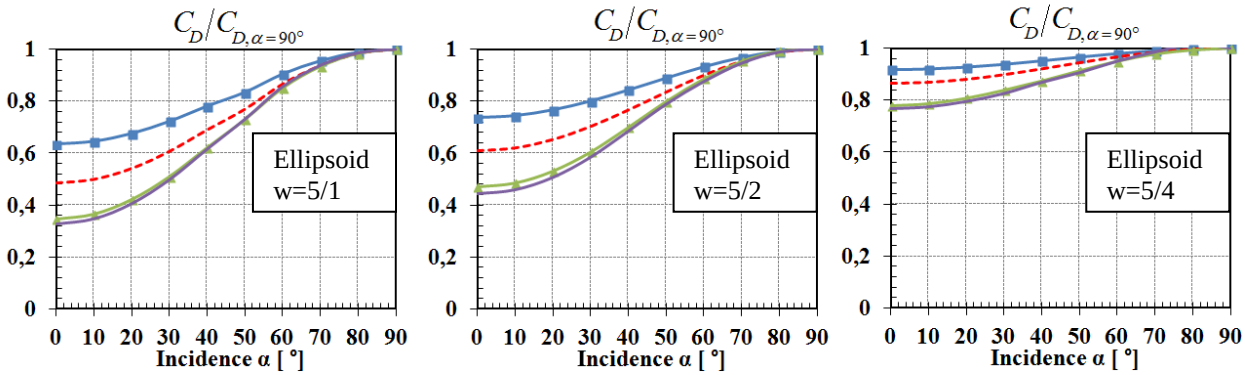

Figure 4. Normalized drag coefficient as a function of the angle of incidence α. ( ): Re_p=10; ( ); Re_p=50; ( ): Re_p =240; ( ): Re_p =300.

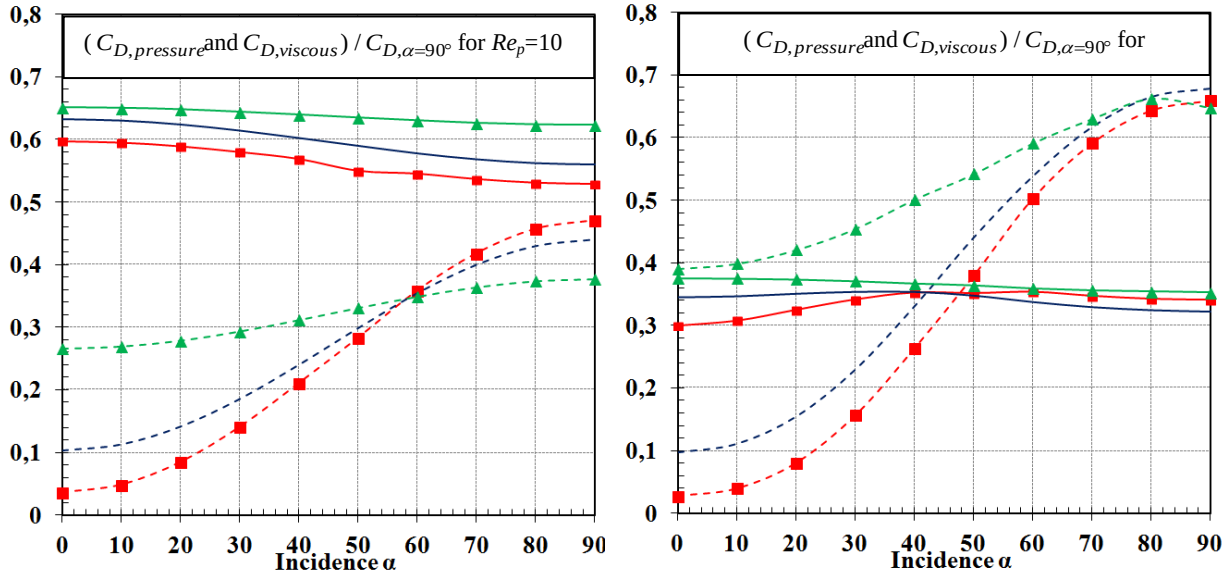

Figure 5. Pressure (dashed lines) and friction (continuous lines) drag coefficients versus $C_{D,\alpha=90°}$ as a function of the angle of incidence α for different aspect ratios. ( ): w=5/1; ( ); w=5/2; ( ): w =5/4.

In figure 6, the computed pitching torque coefficient is plotted as a function of α for two aspect ratios and particle Reynolds numbers. These data are compared to the results given by Zastawny *et al.* [8]. It should be kept in mind

that the pitching torque is obtained by the combination of drag and lift forces acting on the center of pressure. Therefore, as expected, the differences between the present results and those given by the correlation of Zastawny *et al.* [8] are of the same order to those already noticed for the drag and lift coefficients. Despite of a deviation of about 30%, we will use the proposal by Zastawny *et al.* [8] since it is the only existing correlation for the particle shape and particle Reynolds number range we are interested in.

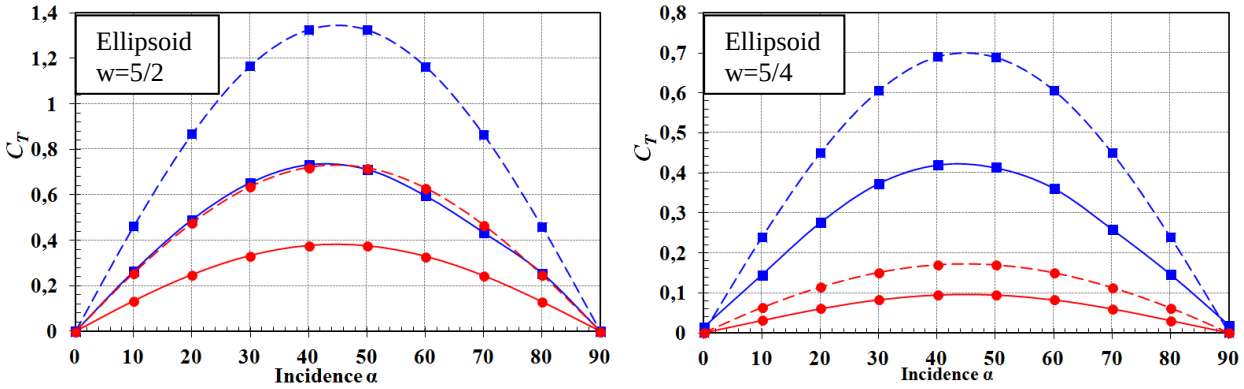

Figure 6. Comparison of the torque coefficients for different particles Reynolds numbers. Present results: (—■—); results of Zastawny *et al.* [8]: (—●—). The dashed lines are referred to $Re_p = 10$ and the continuous lines are referred to $Re_p = 300$.

CONCLUSION

In the present study, we have computed the drag, lift and torque coefficients for ellipsoidal particles as a function of incidence angle and for several values of the particle Reynolds number. These results have been compared to those available in the literature. Firstly, this comparison is not easy since there are few available proposals which predict the whole of coefficients (the drag, lift, and torque coefficients) as a function of the particle orientation, for the particle shapes and range of particle Reynolds number that we want to study. According to the present comparison, our choice will be oriented towards the method of Rosendahl, using Hölzer & Sommerfeld [5] correlation to obtain $C_{D,\alpha=0°}$ and $C_{D,\alpha=90°}$, to predict the drag coefficient. The lift and pitching torque coefficients will be provided by the correlations proposed by Zastawny *et al.* [8], as recently done by Lain & Sommerfeld [14]. The next step will be to introduce these correlations in our DNS/DPS code in order to study the transport of non-spherical particles in wall-bounded turbulent gas-solid flows.

ACKNOWLEDGMENTS

This work received funding by ANR-PLAYER; their support is gratefully acknowledged. We would like to thank our partners IMFT and I2M laboratories.

REFERENCES

1. R.Chhabra, L. Agarwal, N. Sinha. *Powder technology*, 101, 288–295, (1999).
2. Ganser G. H. *Powder technology*, 77(2), 143–152, (1993).
3. S. Tran-Cong, M. Gay, E. Michaelides. *Powder Technology,* 139, 21–32, (2004).
4. H.N Yow, A. Salman, M.J Pitt. *Powder technology*, 16, 4, 363-372, (2005).
5. A. Holzer and M. Sommerfeld, *Powder Technology*, 184, 361–365, (2008).
6. H. Wadell, shapes, *Journal of the Franklin Institute*, 217, 459–490, (1934).
7. L. Rosendahl. Applied Mathematical Modelling, 24, 11–25, (2000).
8. L M. Zastawny, G. Mallouppas, F. Zhao, and B. van Wachem, *Int. J. Multiphase flows*, 101, 288–295, (2012).
5. C.G Yin., L. Rosendah, S.K. Kaer, & H. Sorensen. *Chemical Engineering Science*,58, 15, 3489-3498, (2003).
10. S.F. Hoerner, *Hoerner Fluid Dynamics*, (1965).
11. B.J. Lázaro and J.C. Lasheras, *Physics of Fluids* A, 1, 6, 1035-1044, (1989).
12. S. V. Patankar, Mc Graw Hill Company, ISBN 0891165223 (1980).
13. H. Brenner. *Chemical Engineering Science*, 18, 1-25, (1963).
14. S. Lain and M. Sommerfeld, *8th International conference on Multiphase Flow ICMF* (2013).